



## Simulation of Weather Radar Products from a Mesoscale Model

D. Meetschen<sup>1</sup>, S. Crewell<sup>1</sup>, P. Gross<sup>1</sup>, G. Haase<sup>1</sup>, C. Simmer<sup>1</sup> and A. van Lammeren<sup>2</sup>

<sup>1</sup>Meteorological Institute, Bonn, Germany

<sup>2</sup>KNMI, De Bilt, The Netherlands

Received 14 June 2000; accepted 6 July 2000

**Abstract.** A radar simulation tool (RST) was developed to perform simulations of radar measurements on output data of the Lokal-Modell (LM) of the German Weather Service (Deutscher Wetterdienst, DWD). The LM is an operational non-hydrostatic weather forecast model on the meso- $\gamma$ -scale. Knowing the characteristics of a particular radar (geographic position and hardware parameters) a pseudo measurement can be calculated and typical radar scan patterns (azimuth and elevation scans) can be simulated. The model takes into account atmospheric refraction, attenuation by gases and hydrometeors, and backscattering from different types of hydrometeors simulated by the LM. Additionally, the radar antenna function is explicitly considered.

Because the RST output is similar to real radar data, it can be processed in the same way. We generated rainrate composites for a weather radar network, a standard product in the daily work of forecasters. It can be used for an easy comparison between radar measurements and LM forecasts. A case study simulating the composite of the Dutch radar network for a cold front event is presented.

© 2000 Elsevier Science Ltd. All rights reserved.

### 1 Introduction

The horizontal resolution of numerical weather prediction (NWP) models has increased with time mainly due to the availability of increased computer power. In the future, models operating on the meso- $\gamma$ -scale will be used for severe weather prediction in operational environments. An example is the Lokal-Modell (LM) of the German Weather Service (DWD), which is run operationally with 7 km resolution since 1999. A further increase in resolution to 2.8 km is scheduled for operational use in 2001. For this kind of model the standard synoptic observations are not sufficient for the evaluation of the predicted precipitation. However, existing weather radars as operated within networks by the national weather services have a comparable horizontal res-

olution and can cover the complete model domain.

Unfortunately the accuracy of the rain rate  $R$  derived from the radar reflectivity factor  $Z$  using the conventional relation of the form  $Z = aR^b$  suffers from several problems. Besides the assumption about the drop size distribution (DSD) of the rain particles, errors can arise due to the radar measurement process where the backscattered and attenuated signal from a certain volume at a certain height is measured. To investigate the errors evident in the radar-rainfall measurement Anagnostou and Krajewski (1997) simulated radar measurements from a stochastic space-time rainfall model. Their model includes the effects of statistical parameterized DSD, the antenna beam pattern, the subgrid variability within the measured volume, and random noise in the measurement.

Instead of statistically generated atmospheric fields Haase and Crewell (2000) used three-dimensional fields as predicted by the LM to simulate standard radar products like PPI (plan position indicator) and RHI (range height indicator) as measured by an arbitrary radar located in the LM domain. These products can then be used for a quick validation of the NWP model forecast with similar products from the radar network. The comparison between reflectivity values has two advantages: First, several parameters simulated by the LM contribute to the evaluated product due to the explicit consideration of the beam propagation and the simulation of the backscattered attenuated signal by different hydrometeor types. This leads to an integral assessment of the whole NWP model prediction and not of only one parameter (e. g. the rain rate). Second, some of the errors, which are inherent in the radar-derived precipitation (for example the transformation of a measurement at a certain height to the ground level) are avoided.

In this work an enhanced version of the radar simulation model (RSM) developed by Haase and Crewell (2000), which explicitly takes into account the antenna weighting function, is used to compare weather radar products with a LM forecast. The understanding of the radar measurement process (section 2) and the forecast from the Lokal-Modell (section 3) are the basics needed for the radar simulation tool

Correspondence to: D. Meetschen

(RST) described in section 4. Nowadays forecasters mostly work with so-called composites, which comprise the measurements of several radars within a network. The method to generate composites from the simulations and the measurements is explained in section 5. The results for a case study with the Dutch radar network are presented in section 6.

## 2 Radar measurement process

The average power  $\bar{P}_r$  received by a radar from a target volume centered at position vector  $\vec{r}_0$  can be described by the radar equation (Doviak and Zrnić, 1992):

$$\bar{P}_r(\vec{r}_0) = C_R \int_0^{r_{max}} \int_0^\pi \int_0^{2\pi} \frac{\eta(\theta, \phi, r)}{r^4} l^2 f^4(\theta, \phi) W(\vec{r}_0 - \vec{r}) dV \quad (1)$$

The volume integral ( $dV = r^2 dr \sin \theta d\theta d\phi$ ) is given by the target's distance  $r$  from the radar along the main beam axis, and the two angles  $(\theta, \phi)$  relative to this axis. The coefficient  $C_R$  depends on radar system parameters such as power transmitted, antenna gain, and radar wavelength.  $\eta$  is the reflectivity from hydrometeor scatterers and is integrated over the contributing region weighted by the antenna pattern  $f(\theta, \phi)$  and the range weighting function  $W(\vec{r}_0 - \vec{r})$ , and  $l$  is the one-way loss factor due to atmospheric attenuation.

Equation (1) can be simplified assuming that most contributions to  $\bar{P}_r$  come from a small volume of almost cylindrical shape at range  $r_0$  (absolute value of position vector  $\vec{r}_0$ ):

$$\bar{P}_r(\vec{r}_0) = \frac{C_R l^2}{r_0^2} \int_{r_0 - \frac{1}{2}\Delta r}^{r_0 + \frac{1}{2}\Delta r} \int_0^{2\theta_1} \int_0^{2\pi} \eta(\theta, \phi, r) f^4(\theta, \phi) dV \quad (2)$$

In equation (2) we have assumed a pulsed radar with  $W(\vec{r}_0 - \vec{r})$  a square function given by the pulse length  $\Delta r = \frac{c\tau}{2}$ .  $c$  is the velocity of light and  $\tau$  the pulse duration. The integration volume in equation (2) increases with  $r_0^2$ .

A good approximation for the antenna pattern is in most cases a symmetric Gaussian function where the angle  $\theta_1$ , the so-called full width at half maximum (FWHM), describes the width of the beam. Typically the integration is performed only within this 3-dB contour including only 50 percent of the considered power within the integral. To include nearly all contributions (more than 99 percent) we perform the integration within the  $2\theta_1$  bounds.

Equations (1) and (2) ignore the propagation of radar beams along curved lines caused by variations of the refractive index of the atmosphere. A parameterization for the refractive index of air is given by Doviak and Zrnić (1992):

$$n = 1 + 10^{-6} \left( \frac{77.6}{T} \cdot \left( p + \frac{4810 \cdot p_w}{T} \right) \right) \quad (3)$$

with  $T$  the temperature in K,  $p$  the pressure, and  $p_w$  the partial pressure of water vapor both in hPa. If these fields are

known, the path of an electromagnetic wave through the atmosphere can be calculated on the basis of Snell's law.

## 3 Lokal-Modell

The recent version of the RST uses output of the Lokal-Modell (Doms and Schättler, 1998) of the German weather service as input. It is a non-hydrostatic model on the meso- $\gamma$ -scale. In the version used, the horizontal grid-spacing is 2.8 km, but it may be lowered down to 1 km. In the vertical the atmosphere is divided into 35 terrain-following  $\sigma$ -levels with increasing density towards the ground. The initial and boundary fields are provided by the Deutschlandmodell (DM), which is a hydrostatic mesoscale model with 14 km grid size. The prognostic variables are the wind vector, temperature, pressure perturbation, specific humidity  $q_v$ , and cloud liquid water  $q_c$ , while the geopotential height, rain  $pr_r$  and snow flux  $pr_s$  are diagnostic parameters. Because of the simplified parameterization of precipitation inside the LM some assumptions are necessary, e. g. the shape of the drop size distribution. A detailed description of how the LM fields are adapted in the simulation process is given by Haase and Crewell (2000).

## 4 Radar simulation tool

Figure 1 illustrates, how the radar simulation tool works. Of course the fields provided by the LM are meteorological parameters, of which only a few influence more or less the power received by the antenna. In a first step, RST converts the three dimensional LM fields of rain flux and snow flux, specific humidity, cloud water content, temperature, and pressure into fields of specific reflectivity  $\eta$ , specific attenuation  $K$  and refractivity  $n$ .

The illuminated volume described by the integral in equation (2) is small compared to the LM resolution. For an accurate integration, it is necessary to have an appropriate number of grid points within the considered sampling volume. Thus, the interface procedure interpolates the calculated values of reflection, attenuation and refractivity onto a high-resolution grid. For a typical radar system with a FWHM of  $1^\circ$  and a pulse-length of  $2 \mu s$ , for example, the resolution should not be larger than a few hundred meters. The high-resolution grid has cartesian coordinates with  $x = y = 0$  at the antenna position and  $z = 0$  on sea level.

The actual simulation of the radar measurement proceeds like a real radar measurement through a given number of antenna positions usually following a typical scan pattern. For each antenna position RST starts with calculating the path of the radar beam to the first range bin. The curvature of the beam due to the gradient of refractivity is imitated by refracting it at the boundaries of the horizontal layers of the high-resolution grid. To allow anomalous propagation, total reflection is included in this procedure. Assuming, that horizontal gradients of refractivity are insignificantly small,

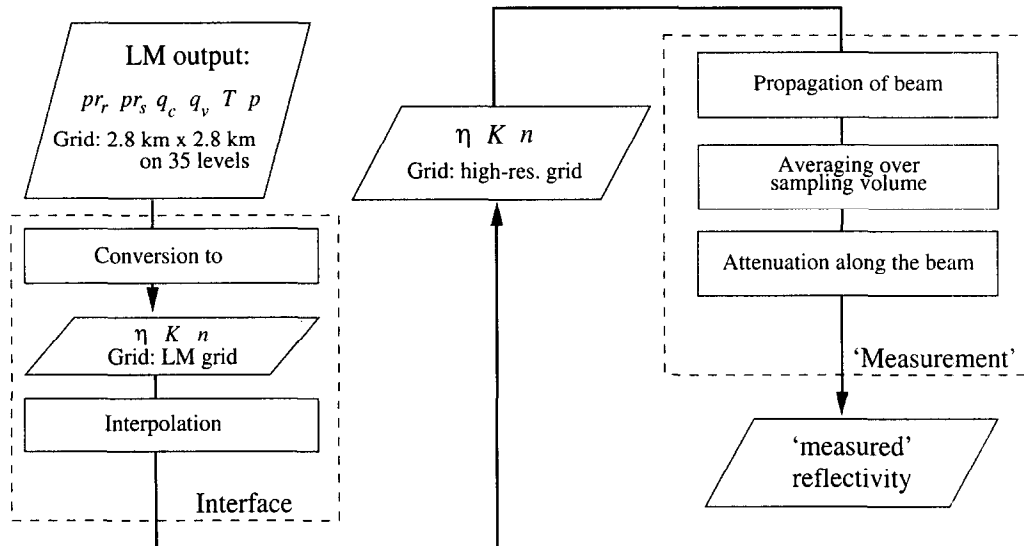


Fig. 1. Flowchart of RST: The interface procedure provides reflectivity, attenuation and refractivity fields on a high-resolution grid for the actual simulation process.

refraction at vertical box boundaries is neglected.  $\theta_1$  in equation (2) is so small that the illuminated volume can be approximated by a cylinder with radius  $r_0 \tan 2\theta_1$  and length  $\Delta r$ . For every point of the high-resolution grid inside the cylinder the angle distance from the beam axis is calculated as input for the axis symmetric antenna function (here assumed to be Gaussian). These weighting factors are used to calculate the reflectivity and specific attenuation as average over the grid points inside the cylinder. This procedure is performed for each range bin. The specific attenuation is multiplied with the length of the path from the last range bin to get the attenuation  $l_i$  on that path. The attenuation for range bin  $i$  on the whole path from the antenna and back is

$$l^2 = \prod_{j=1}^{i-1} l_j^2. \quad (4)$$

The result of this procedure is the reflectivity factor for all range bins of all the requested antenna positions.

The main improvement to the RSM of Haase and Crewell (2000) is the explicit consideration of the antenna weighting function. Unlike the pencil beam used before RST takes into account that each single radar measurement is representative for a volume, so that gradients of reflectivity are smoothed out. Simulating this effect does not only provide more realistic images of structures like bright-band but can also eliminate small scale model artifacts.

## 5 Compositing

To obtain precipitation measurements over a larger area, real radar data of a volume scan are typically processed into a so-called pseudo-CAPPI<sup>1</sup> and data of several radars are combined into a composite. The same procedure has to be car-

Parameter	Value for KNMI systems
Number of rays per PPI	360
Number of range bins per ray	1360
Pulse length	2 $\mu$ s
Wavelength	5 cm
Digitizing frequency	600 kHz
Geographic coordinates of radar systems	52.1027 N, 5.1785 E <sup>1</sup> 52.3050 N, 4.7557 E <sup>2</sup>
Height above sea level of radar systems	44.1 m <sup>1</sup> 43.0 m <sup>2</sup>
FWHM of antenna function	1.0°

Table 1. Parameters needed by RST (<sup>1</sup>De Bilt, <sup>2</sup>Schiphol)

ried out with the simulated data as well, if it should be compared with real data. The comparison in section 6 is made for the Dutch radar network (Wessels, 1995) operated by KNMI. The pseudocappi composite is based on volume scans of two radar systems in the Netherlands. The radar positions and hardware parameters necessary for the RST are given in Table 1.

Each volume scan contains four PPIs at elevations of 0.3°, 1.1°, 2.0° and 3.0°. First, each of them is interpolated onto a rectangular grid of 0.1° × 0.1° resolution. The pseudocappi of reflectivity for a single radar at a height  $h$  is calculated by a linear interpolation between the two next measurements below and above  $h$ , respectively. If all of the measurements are below  $h$  or all above  $h$ , simply the closest one is taken. Figure 2 shows the positions where the single PPIs intersect the pseudocappi height  $h = 1$  km. It is obvious that the two radars located in De Bilt and Schiphol do not cover the area of the Netherlands in an optimal way. Nowadays the Schiphol radar is not in operation anymore and a new radar is operated at Den Helder (52.9 N, 4.8 E) leading to a better coverage. However, for the case study presented in section 6 Schiphol was still in use.

<sup>1</sup>Constant Altitude PPI

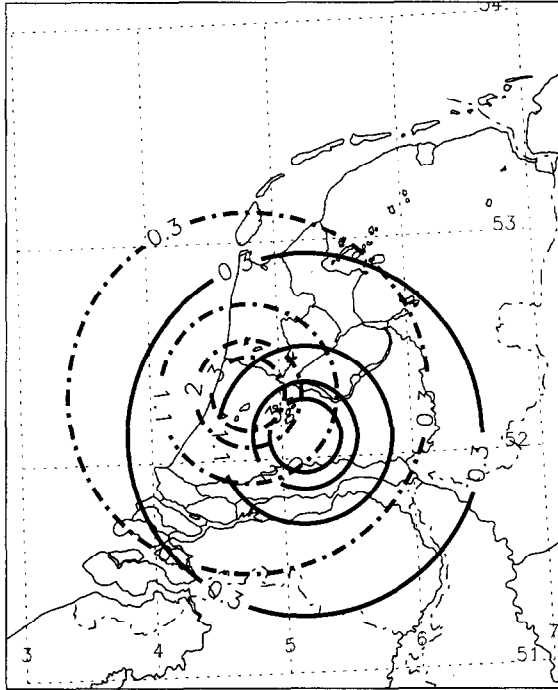


Fig. 2. Locations where the four single azimuth scans within a volume scan intersect the 1 km pseudocappi level for the radar at De Bilt (solid) and Schiphol (dashed dotted).

The compositing procedure in general takes the maximum of the values from all given radar systems at every single pixel of the picture. If one or more other radars are close to a radar A (less than 120 km), the data of A is neglected inside a circle of 15 km radius around A to avoid problems with clutter in that area. From a range of 15 to 40 km the measurements from A are increasingly taken into account, to prevent artifacts in the picture.

## 6 Case Study

For comparison we selected the 26 January 1995 when a cold front approached the Netherlands from north-west. The strong precipitation connected with this system contributed strongly to the flooding event in the lower Rhine area. The LM was initialized with an analysis of the Deutschlandmodell (DM) at 00:00 UTC. The forecasted fields for 13:00 UTC were input to the RST to simulate the volume scans of the two Dutch radars in De Bilt and Schiphol, which were then used for the compositing as described in the previous section.

Figure 3 shows the resulting composite and the corresponding measurement of the Dutch radar system at this time. Both composites show an intense frontal band of about 200 km length close to the eastern border of the Netherlands. While in the observation a second, shorter band is trailing this main band in the southern part of the Netherlands, the LM simulation shows these kind of lines before the front.

The larger stratiform precipitation areas in the north are also depicted by the LM. The wave-like structures with a wavelength of about 15 km in the north-east of the LM composite are artifacts due to the mesoscale model. Unlike small scale artifacts these can not be smoothed away by the antenna averaging which is done in volumes of 600 m length and up to 5 km diameter.

## 7 Summary

A radar simulation tool was presented, which can be used to generate weather radar products like PPI and RHI from forecasts of a mesoscale model. For a cold front system passing the Netherlands on 26 January 1995 the volume scans of two Dutch radars were simulated. A composite image was generated in the same manner as it is operationally done with the real measurements. The comparison between both composites shows a quite successful forecast of this frontal event. To quantify the visible impression objective skill scores should be used as in Haase and Crewell (2000). This should be done not only for one point in time but also over the whole forecast period. Hence, the RST is a tool which can easily be adapted to the operational evaluation of NWP forecasts. This is already done by the German Weather Service in the ongoing validation of the LM by generating PPIs with the RSM for single radar sites. The study presented here has shown the potential in generating composite products for a whole network. The RST will be updated in the future to include current developments in the LM, e.g. the inclusion of ice mass flux as a prognostic variable.

*Acknowledgements.* The authors thank Herman Wessels from KNMI for providing the information on the Dutch radar network.

## References

- Anagnostou, E. N. and Krajewski, W. F., Simulation of radar reflectivity fields: Algorithm formulation and evaluation, *Water Resources Research*, 33, 1419–1428, 1997.
- Doms, G. and Schättler, U., *The nonhydrostatic limited-area model LM (Lokal-Modell) of DWD, Part I: Scientific documentation*, German Weather Service (DWD), Research Department, P. O. 10 04 65, D-63004 Offenbach, 160p, 1998.
- Doviak, R. J. and Zrnić, D. S., *Doppler radar and weather observations*, Academic press, Inc., San Diego, California, second edn., (ISBN 0-12-221422-6), 1992.
- Haase, G. and Crewell, S., Simulation of radar reflectivities using a mesoscale weather forecast model, *Water Resources Research*, accepted, 2000.
- Wessels, H. R. A., Stepwise procedure for suppression of anomalous ground clutter, in *COST 75 - Weather Radar Systems*, edited by C. G. Collier, pp. 270–277, European Commission, Office for Official publications of the European Communities, 1995.

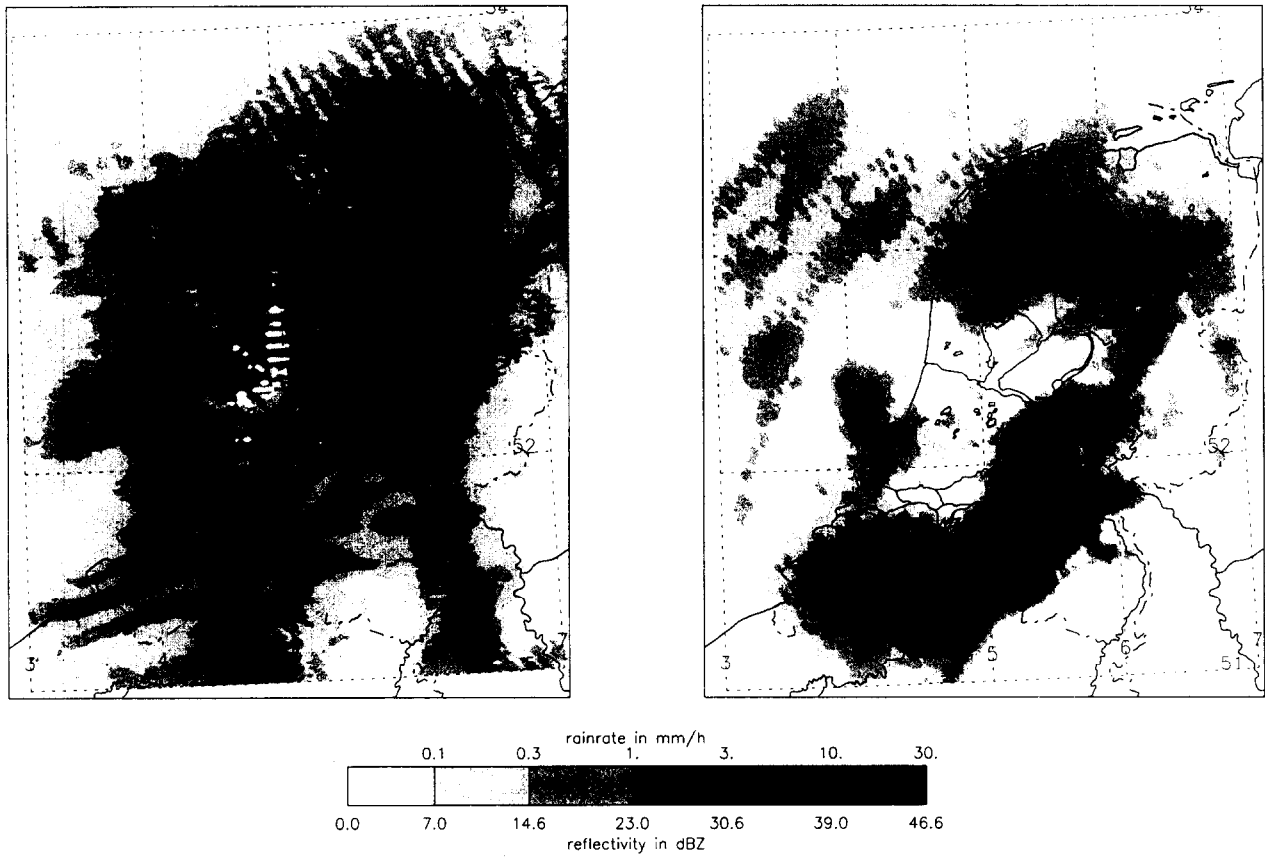


**Fig. 3.** Composite of LM simulations (left) and the corresponding measurements (right) of KNMI radars for 26 January 1995 13:00 UTC.